Calculation of Fluxgate Sensor Parameters

İlker Yağlıdere[1,2] and Ece Olcay Güneş[1]

[1]Electronics and Communication Engineering Department, Istanbul Technical University, Istanbul, 34469, Turkey
iyaglidere@gmail.com, gunesec@itu.edu.tr
[2]ASELSAN Electronics Inc., 296. Street, 06370, Ankara, Turkey

Abstract

In this work, we present two ring-core fluxgate sensor designs to investigate the accuracy of parameter calculations such as inductance and resistance of the windings, demagnetization factor and apparent permeability. All these parameters as well as relative permeability are measured and some simulations are performed through a FEM (Finite Element Method) analysis tool. Measurement results are compared with the calculated theoretical values in addition to FEM analysis results. In the first design, a crystalline core stacked from circular permalloy laminations is used while an amorphous core wound from Vitrovac 6025Z strip is preferred for the second design. Demagnetization factors are calculated by using well-known empirical and analytical formulas in the literature. The results point out that a new demagnetization factor formula is necessary because the three formulas used miscalculate for the designed sensors. Moreover, calculating the demagnetization factor by using finite element analysis method is found to be reliable.

1. Introduction

Fluxgate sensors have come a long way since Aschenbrenner and Goubau started to construct the first fluxgate magnetometer in 1928 and published their paper in 1936 [1]. Sensitive sensors were designed for ship and submarine detection during the Second World War [2]. After the war, they have been widely used as compasses in shipping and aviation as well as in rocket and missile systems [3]. The Soviet research satellite Sputnik 3 launched in 1958 was the first space application of fluxgates [4]. Since 1980s, fluxgates have been used for observing the variations in Earth's magnetic field [5]. Starting with 1990s, micro-fluxgates were developed, but they suffer from low sensitivity and high noise [6]. Sweden's second microsatellite Astrid-2 with a digital fluxgate payload was launched in 1998 to explore the electric and magnetic fields in the upper ionosphere [7]. In 1999, Denmark's first satellite Ørsted was launched for mapping the earth's field [8]. NASA used fluxgates in THEMIS satellite in 2007 [9]. By 2015, NASA started the "Magnetospheric Multiscale Mission" comprising four identically instrumented spacecrafts equipped with ASIC fluxgates, to study the microphysics of magnetic reconnection by using Earth's magnetosphere as a laboratory [10]. One of the recent applications is precise electric current sensing. Texas Instruments announced the DRV421 and DRV425 CMOS integrated fluxgate sensors specified for operation over the extended industrial temperature range of -40°C to +125°C in 2015 and they can replace the classical Hall probes [11, 12].

Since the most popular geometries suffer from high demagnetization effect which limits the sensitivity and increases the sensor noise, calculating demagnetization factor accurately becomes more of an issue. Many empirical formulas [13, 14] and an analytical formula [15] have been proposed for the ring-core, but none of them succeeds for a wide range of dimensions. For example, the proposed formula in [13] was validated for only four cores having identical diameter and height values. If a fluxgate is to be designed with a commercial strip wound core, relatively thick cores in the market are the only alternative. The fluxgate output voltage formula and the effect of demagnetization factor on the output voltage are given in [16]. The first goal of this study is measuring the demagnetization factors of the two ring-core sensors designed and comparing them with the values calculated by using three well-known formulas. The second goal is performing some finite element analyses to investigate the formulas. Finally, we aim to examine the consistency of current formulas. Physical design details are described in Section II. Sections III and IV give the calculation and measurement results while Section V concludes with the comparison of the results.

2. Physical Design and Dimensions

A fluxgate core stacked from four circular permalloy laminations is used in the first design (sensor-1) while a core wound from 45 turns of 19 µm thick Vitrovac 6025Z strip is used in the second design (sensor-2). The physical dimensions of the sensors are tabulated in Table 1 and some mechanical details are illustrated in Fig. 1.

Table 1. Physical dimensions of the sensors

Dimension	Symbol	Sensor-1 mm	Sensor-2 mm
lamination thickness	$t_{lamination}$	0.3	-
strip thickness	t_{strip}	-	0.019
outer diameter (bare)	OD_{bare}	12.17	10.00
inner diameter (bare)	ID_{bare}	8.81	8.00
height (bare)	h_{bare}	1.20	3.80
outer diameter (boxed)	OD_{boxed}	13.65	11.60
inner diameter (boxed)	ID_{boxed}	7.70	6.50
height (boxed)	h_{boxed}	2.80	5.10
excitation coil wire dia.	d_{exc}	0.20	0.20
pickup coil wire dia.	d_{pickup}	0.40	0.14
pickup coil length	l_{pickup}	15.10	13.38
pickup coil width	w_{pickup}	20.00	16.30
pickup coil height	h_{pickup}	5.0	6.5

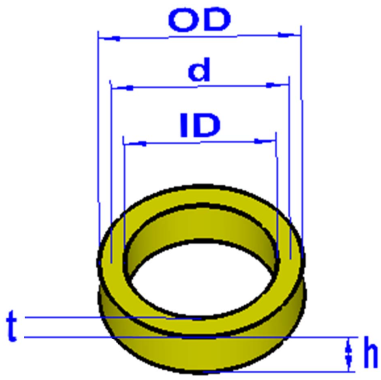

Fig. 1. Core dimensions

Support material used in sensor-1 is shown in Fig. 2. In this configuration, the toroidal core close fits to the support material and the structure is mechanically stable, which makes it ideal for commercial sensors.

Sensor-2 is produced with a different support geometry, which allows inserting and removing the core easily through the support. When using such a configuration, it is easy to measure the pickup coil inductance with and without the core; therefore, it is appropriate for scientific studies. Sensor-2 is shown in Fig. 2 and some parameters of the designed sensors are tabulated in Table 2.

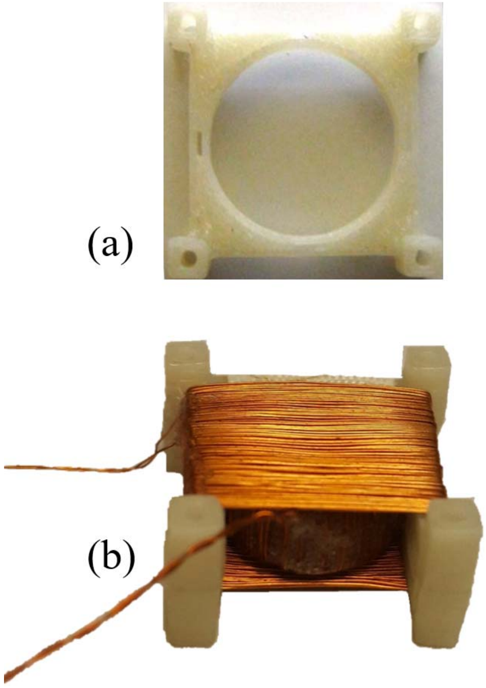

Fig. 2. Support material for (a) sensor-1 and (b) sensor-2

3. Relative Permeability Measurements

Relative permeability measurements are performed by measuring the inductance of the excitation coils (L_{exc}) at near DC (100Hz) with a Keysight U1733C handheld LCR meter. The permeability values are then calculated from the measured inductance values. By assuming that a non-significant demagnetizing field occurs for the circular excitation field along the toroidal core and it can be neglected, the calculated effective permeability (μ_{eff}) values are accepted as relative permeability (μ_r) values. The following general equations are used for excitation coil inductance and path length calculations:

$$L_{exc} = \frac{\mu_0 \mu_r N_{exc}{}^2 A_{core}}{l_{path}}, \tag{1}$$

$$l_{path} = \frac{\pi(OD_{bare} - ID_{bare})}{\ln(\frac{OD_{bare}}{ID_{bare}})}, \tag{2}$$

where bare dimensions and N_{exc} represent the dimensions of the core without the plastic case and excitation coil turn number, respectively. The effective path length (l_{path}) is not calculated by directly averaging the inner and outer circumferences. Because the flux lines inside the toroidal core concentrate in the shorter paths, the effective path length is somewhat smaller than the average circumference. Although it has a minor effect on the path length for thin ring-cores, it is not neglected in calculations. Measured relative permeability values are given in Table 2.

Table 2. Some important parameters of the designed sensors

Parameter	Symbol	Unit	Sensor-1	Sensor-2
material	-	-	permalloy	6025Z
path length[a]	l_{path}	mm	32.67	28.16
cross sectional area	A_{core}	mm^2	2.016	3.20
resistance of unit length	σ_{exc}	mΩ/m	538.3	538.3
winding number	N_{exc}	turns	102	86
coil inductance[b]	L_{exc}	mH	15.82	26.71
relative permeability[c]	μ_r	-	19610	25288
cross sectional area	A_{pickup}	mm^2	100.00	105.95
resistance of unit length	σ_{pickup}	mΩ/m	168.9	1079
winding number	N_{pickup}	turns	36	78

[a]calculated by using (2).
[b]measured.
[c]calculated from the measured coil inductance.

4. Calculations and Measurement Results

Coil resistances are calculated by multiplying the wire length (l_{wire}, in mm) with the wire resistivity per unit length (σ). For excitation coils, wire length is calculated as

$$l_{wire} = N_{exc} l_{1-turn} + 200 \\ = N_{exc}\left[\left(OD_{boxed} - ID_{boxed}\right) + 2h_{boxed} + 4d_{exc}\right] + 200. \quad (3)$$

For pickup coils, wire length is calculated as

$$l_{wire} = N_{pickup} l_{1-turn} + 200 \\ = N_{pickup}\left[2\left(w_{pickup} + h_{pickup}\right) + 4d_{pickup}\right] + 200. \quad (4)$$

The term 200 in (3) and (4) is the length of wire outside the coil. Apparent permeability is calculated by using the measured inductance values:

$$\mu_a = \frac{L_{pickup} - L_{air}}{L_{air}} \frac{A_{pickup}}{2A_{core}} + 1. \quad (5)$$

When μ_r and μ_a are known, then global demagnetization factor D_{global} can be found as follows [13]:

$$D_{global} = \frac{\mu_r - \mu_a}{\mu_a(\mu_r - 1)}. \quad (6)$$

Pickup coil inductance without the core is calculated as

$$L_{air} = k_{non-uniformity} \frac{\mu_0 N^2 A_{pickup}}{l_{pickup}}, \quad (7)$$

in which $k_{non-uniformity}$ is a magnetic field non-uniformity correction factor (also known as Nagaoka's coefficient). Nagaoka's coefficient is generally between 0.7 and 0.95 for pickup coils and always smaller than 1. The constant can be calculated precisely by using Lundin's handbook formula [17] for coils with a circular cross section. Some approximations can be used for coils with a rectangular cross section. In this study, $k_{non-uniformity}$ values are calculated by using the measured L_{air} values. Inductance of the pickup coil with core is calculated as follows:

$$L_{pickup} = k_{non-uniformity} \frac{\mu_0 N^2}{l_{pickup}}\left(A_{pickup} + 2(\mu_a - 1)A_{core}\right). \quad (8)$$

Demagnetization factor is calculated using the following well-known formulas in which t, d and A denote core thickness, average core diameter and cross sectional core area, respectively [13-15]:

$$D_{global} = 0.223\frac{t}{d}, \quad (9)$$

$$D_{local} = 1.83\frac{A}{d^2}, \quad (10)$$

$$D_{local} = \frac{1}{\pi}\left\{\ln\left[\left(\frac{4(d+t)}{h}\right)^2\right] - 1\right\}\frac{A}{(d+t)^2}. \quad (11)$$

Measured values in addition to the calculated values by using the given formulas and FEM analysis software are tabulated in Table 3. Demagnetization factor, apparent permeability and the pickup coil inductance are the parameters that are difficult to be calculated as seen in Table 3.

Table 3. Comparison of the measured and calculated values for the sensors designed

Parameter	Unit	Sensor-1 Measured	Sensor-1 Calculated	Error %	Sensor-2 Measured	Sensor-2 Calculated	Error %
R_{exc}	Ω	0.82	0.79	-3.66	0.86	0.85	-1.16
R_{pickup}	Ω	0.27	0.26	-3.70	4.00	4.10	+2.50
L_{air}	mH	9.1	9.1	0.00	56.0	56.0	0.00
$k_{non-uniformity}$	-	0.844	-	-	0.925	-	-
L_{pickup}	µH	18.00	19.00[a]	+5.55	99.0	214.5[a]	+117
			14.20[b]	-21.1		76.00[b]	-23.2
			15.34[c]	-14.8		96.33[c]	-2.70
			17.07[d]	-5.18		94.62[d]	-4.43
D_{global}	-	0.0395	0.0357[a]	-9.69	0.0729	0.0209[a]	-71.4
			0.0671[b]	+69.7		0.1446[b]	+98.4
			0.0556[c]	+40.5		0.0773[c]	+6.11
			0.0440[d]	+11.3		0.0805[d]	+10.4
μ_a	-	25.26	27.96[a]	+10.7	13.71	47.84[a]	+249
			14.89[b]	-41.0		6.91[b]	-49.6
			17.98[c]	-28.8		12.92[c]	-5.76
			22.70[d]	-10.1		12.42[d]	-9.44

[a]Calculated by using the empirical formula D_{global}=0.223(t/d).
[b]Calculated by using the empirical formula D_{local}=1.83(A/d^2) and (12).
[c]Calculated by using the analytical formula given in (11) and (12).
[d]FEM analysis results.

The following relation can be used for transition between local and global demagnetization factors in a ring-core fluxgate [14]:

$$D_{global} = 2D_{local} + \frac{1}{\mu_r - 1}. \quad (12)$$

For high values of μ_r, the second term can be neglected.

Pickup and excitation coil resistances as well as pickup coil inductances without the core are calculated precisely. However, calculated demagnetization factor and related parameter (e.g. pickup coil inductance and apparent permeability) values are quite different from the measured values. These differences are all caused by the errors in demagnetization factor calculations. For both sensors designed, (9) underestimates the demagnetization factor, whereas (10) and (11) overestimate the factor. In contrast to the three formulas, FEM analyses overestimate with an error about only 10% as shown in Table 3.

5. Discussion and Conclusions

Two ring-core fluxgate sensors made of amorphous and permalloy materials are presented. Demagnetization factors are measured and compared with the values calculated by using the three popular formulas and quite different demagnetization factor values are observed. The measurement results are validated by FEM analyses. It is concluded that the two most widely used demagnetization factor formulas proposed by Primdahl et al. in 1989 and 2002 as well as the analytical formula proposed by M. De Graef et al. in 2006 are not valid for the tested dimensions. Great care should be taken while using these empirical and analytical formulas by keeping in mind that they can lead to error levels above 90% and 40%, respectively. The results show that finite element analysis tools offer the most reliable solutions.

Fluxgate demagnetization factor should be calculated accurately before production because it is the most important design parameter, which determines both sensor noise and sensitivity. Despite being over 80 years since Aschenbrenner and Goubau have presented the very first fluxgate magnetometer, a reliable demagnetization factor formula for ring-core fluxgate is still absent. We strongly suggest using finite element analysis tools for calculating the demagnetization factor and related parameters instead of using the current demagnetization factor formulas. A second study is planned to further analyze the demagnetization phenomenon and propose a novel method for calculating the demagnetization factor.

6. Acknowledgment

We wish to thank Aktif Neser Elektronik Ltd. Sti. and CST - Computer Simulation Technology AG for supporting this research by supplying a demo license for CST EM STUDIO.

7. References

[1] H. Aschenbrenner and G. Goubau, "Eine anordnung zur registrierung rascher magnetischer störungen", *Hochfreq. Electroakustik*, vol. 47, no. 6, pp. 177-181, Jun., 1936.

[2] H. How and C. Vittoria, "Generation of high-order harmonics in insulator magnetic fluxgate sensor cores", *IEEE Trans. Magn.*, vol. 37, no. 4, pp. 2448-2450, Jul., 2001.

[3] A. Grosz, M. Janosek, Haji-Sheikh and S. C. Mukhopadhyay, eds., "High Sensitivity Magnetometers", Springer, Switzerland, 2017.

[4] K. Shirae, "Noise in amorphous magnetic materials", *IEEE Trans. Magn.*, vol. 20, no. 5, pp. 1299-1301, Sep., 1984.

[5] R. Langel, et al., "The MAGSAT mission", *Geophys. Res. Lett.*, vol. 9, no. 4, pp. 243-245, Apr., 1982.

[6] Y. Liu, et al., "Improved performance of the micro planar double-axis fluxgate sensors with different magnetic core materials and structures", *Microsyst. Technol.*, vol. 22, no. 9, pp. 2341-2347, Sep., 2016.

[7] E. B. Pedersen, et al., "Digital fluxgate magnetometer for the Astrid-2 satellite", *Meas. Sci. Technol.*, vol. 10, no. 11, pp. N124, Nov., 1999.

[8] O. V. Nielsen, et al., "Development, construction and analysis of the 'OErsted' fluxgate magnetometer", *Meas. Sci. Technol.*, vol. 6, no. 8, pp. 1099, Aug., 1995.

[9] H. U. Auster, et al., "The THEMIS fluxgate magnetometer" in "The THEMIS Mission", Springer, New York, 2009.

[10] C. T. Russell, et al., "The magnetospheric multiscale magnetometers", *Space Sci. Rev.*, vol. 199, no. 1-4, pp. 189-256, Mar., 2016.

[11] M. F. Snoeij, et al., "An integrated fluxgate magnetometer for use in closed-loop/open-loop isolated current sensing" in *European Solid-State Circuits Conference*, Graz, Austria, 2015, pp. 263-266.

[12] M. F. Snoeij, et al., "Integrated Fluxgate Magnetometer for Use in Isolated Current Sensing", *IEEE J. Solid-State Circuits*, vol. 51, no. 7, pp. 1684-1694, Jul., 2016.

[13] F. Primdahl, et al., "Demagnetising factor and noise in the fluxgate ring-core sensor", *J. Phys. E*, vol. 22, no. 12, pp. 1004, Dec., 1989.

[14] F. Primdahl, et al., "The fluxgate ring-core internal field", *Meas. Sci. Technol.*, vol. 13, no. 8, pp. 1248, Jul., 2002.

[15] M. De Graef and M. Beleggia, "The fluxgate ring-core demagnetizing field", *J. Magn. Magn. Mater.*, vol. 305, no. 2, pp. 403-409, Oct., 2006.

[16] İ. Yağlıdere, "A Sensitive Fluxgate Magnetic Sensor Design", M.S. thesis, Elec. and Com. Eng. Dept., Istanbul Tech. Univ., Istanbul, TR, 2010.

[17] R. Lundin, "A handbook formula for the inductance of a single-layer circular coil", *Proc. of the IEEE*, vol. 73, no. 9, pp. 1428-1429, Sep., 1985.